Cancer Letters 448 (2019) 84–93

Contents lists available at ScienceDirect

Cancer Letters

journal homepage: www.elsevier.com/locate/canlet

Original Articles

Crizotinib enhances anti-CD30-LDM induced antitumor efficacy in NPM-ALK positive anaplastic large cell lymphoma

Rong Wang[a,b,1], Liang Li[a,1], Aijun Duan[a], Yi Li[a], Xiujun Liu[a], Qingfang Miao[a,*], Jianhua Gong[a,**], Yongsu Zhen[a]

[a] NHC Key Laboratory of Biotechnology of Antibiotics, Department of Oncology, Institute of Medicinal Biotechnology, Chinese Academy of Medical Sciences & Peking Union Medical College, Beijing, China
[b] Department of Blood Transfusion, The Affiliated Hospital of Qingdao University, Qingdao, Shandong, China

ARTICLE INFO

Keywords:
Antibody-drug conjugate
Anaplastic lymphoma kinase
Targeted therapy
ERK1/2
DNA damage

ABSTRACT

Combining antibody-drug conjugates (ADCs) with targeted small-molecule inhibitors can enhance antitumor effects beyond those attainable with monotherapy. In this study, we investigated the therapeutic combination of a CD30-targeting ADC (anti-CD30-lidamycin [LDM]) with a small-molecule inhibitor (crizotinib) of nucleophosmin-anaplastic lymphoma kinase NPM-ALK in $CD30^+/ALK^+$ anaplastic large cell lymphoma (ALCL). *In vitro*, anti-CD30-LDM showed strong synergistic antiproliferative activity when combined with crizotinib. Furthermore, treatment with anti-CD30-LDM plus crizotinib resulted in a stronger induction of cell apoptosis than monotherapy with either treatment. Western blot analysis revealed that ERK1/2 phosphorylation was increased in response to anti-CD30-LDM-induced DNA damage. Interestingly, the addition of crizotinib inhibited the expression of phosphorylated ERK1/2 and further augmented anti-CD30-LDM-mediated apoptosis, providing a potential synergistic mechanism for DNA-damaging agents combined with NPM-ALK inhibitors. In Karpas299 and SU-DHL-1 xenograft models, anti-CD30-LDM plus crizotinib was more effective in inhibiting tumor growth than either treatment alone. This research demonstrated for the first time that the combination of anti-CD30-LDM and crizotinib exhibits a synergistic inhibitory effect in tumor cells. These results provide scientific support for future clinical evaluations of anti-CD30-LDM, or other DNA-damaging agents, combined with NPM-ALK inhibitors.

1. Introduction

Anaplastic large cell lymphoma (ALCL) is an aggressive form of malignant T-cell lymphoma that accounts for approximately 2% of adult and 10–15% of pediatric/adolescent non-Hodgkin lymphoma cases [1,2]. Although ALCL is a largely curable disease, significant percentages (40–65%) of patients develop recurrent disease after front-line therapy and therefore require subsequent treatments [3]. ALCL patients whose disease relapses after autologous stem cell transplantation are rarely cured with current treatment modalities. ALCL is characterized by the overexpression of the CD30 antigen, which is a transmembrane member of the tumor necrosis factor receptor superfamily [4–6]. Thus, CD30 is an attractive and validated target for antibody-based therapy in ALCL [7,8]. Brentuximab vedotin (BV) is an antibody-drug conjugate (ADC) that specifically delivers the potent cytotoxic drug monomethyl auristatin E (MMAE) to CD30-positive cells. BV is FDA-approved for the treatment of relapsed/refractory Hodgkin lymphoma (HL) and ALCL; however, many patients do not achieve complete remission and eventually become resistant to BV treatment. Furthermore, MMAE resistance has been associated with resistance to BV. Therefore, it is imperative to develop other cytotoxic agents that can be linked to ADCs) [9].

Lidamycin (LDM) is a novel enediyne-containing antitumor antibiotic developed by our laboratory. LDM inhibits DNA synthesis and

Abbreviations: ADC, antibody-drug conjugate; ALCL, anaplastic large cell lymphoma; BSA, bovine serum albumin; BV, Brentuximab vedotin; CDI, coefficient of drug interaction; H&E, hematoxylin and eosin; HL, Hodgkin lymphoma; IC_{50}, half-maximal inhibitory concentration; LDM, Lidamycin; mAb, monoclonal antibody; MMAE, monomethyl auristatin E; NPM-ALK, nucleophosmin-anaplastic lymphoma kinase

* Corresponding author.
** Corresponding author.
E-mail addresses: miaoqf@sina.com (Q. Miao), ann_gong@hotmail.com (J. Gong).
[1] These authors equally contributed to this work.

https://doi.org/10.1016/j.canlet.2019.02.002
Received 29 November 2018; Received in revised form 28 January 2019; Accepted 1 February 2019
0304-3835/ © 2019 Published by Elsevier B.V.

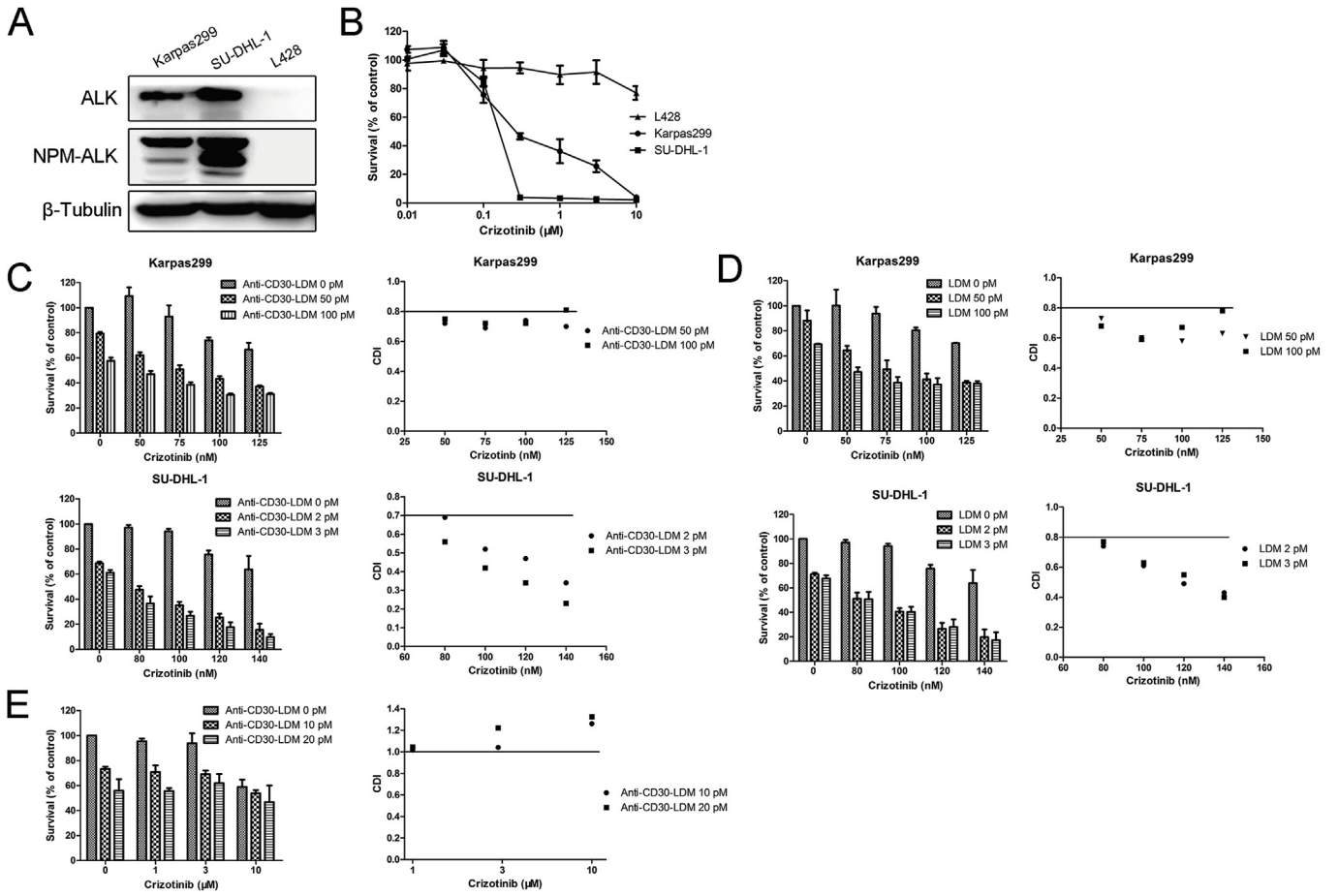

Fig. 1. The cytotoxic effects of crizotinib and/or anti-CD30-LDM on cancer cells. (A) The expression levels of ALK and NPM-ALK in Karpas299, SU-DHL-1, and L428 cells were assessed by western blot. (B) Karpas299, SU-DHL-1 and L428 cells were treated with crizotinib (0.01, 0.03, 0.1, 0.3, 1, 3, or 10 μM) for 48 h, and cell viability was detected by a CCK-8 assay. The survival rates were calculated as the ratios of the optical density of surviving cells in the treatment groups to that in the control group. (C) The synergistic inhibitory effect of the anti-CD30-LDM and crizotinib combination is shown in Karpas299 and SU-DHL-1 cells. The cells were treated with anti-CD30-LDM and/or crizotinib at the indicated concentrations for 48 h. The CDI values were calculated; CDI < 1 indicates a synergistic effect, CDI < 0.7 indicates a significant synergistic effect. The values represent as the mean ± SD of three independent experiments. (D) The synergistic inhibitory effect of the LDM and crizotinib combination is shown in Karpas299 and SU-DHL-1 cells. (E) The effect of anti-CD30-LDM combined with crizotinib on ALK-negative L428 cells; CDI > 1 represents an antagonistic effect.

causes cellular DNA breakage in cancer cells [10]. The chromophore of LDM interacts with the DNA minor groove and cleaves double-helical DNA, causing direct double-strand breaks [11]. We have previously described a novel ADC, anti-CD30-LDM [12], which is comprised of two molecules of LDM linked to an anti-CD30 monoclonal antibody (mAb) via noncleavable linkers. Thus, the LDM is delivered to the CD30-positive cancer cells by the mAb, causes DNA damage by inducing double-strand breaks, and results in cell cycle arrest and apoptosis [13,14]. This ADC displays specific affinity and extremely potent cytotoxicity against CD30-overexpressing tumor cells *in vitro*, with IC_{50} (half-maximal inhibitory concentration) values ranging from 0.54×10^{-11} to 3.74×10^{-11} M. In a Karpas299 xenograft model, tumor growth was inhibited by 87.76% in NOD/SCID mice treated with 0.7 mg/kg anti-CD30-LDM [12]. The combination of ADCs with small molecule inhibitors has been effective in enhancing the antitumor effects of the ADCs [15,16]. Thus, it is important to explore potential combinations of anti-CD30-LDM and small molecule inhibitors that exhibit synergistic antitumor effects.

Anaplastic lymphoma kinase (ALK) is a receptor tyrosine kinase in the insulin receptor family and is expressed in most ALCL cases [17,18]. Nucleophosmin-anaplastic lymphoma kinase (NPM-ALK) is an oncogenic fusion protein carrying the constitutively active tyrosine kinase and is expressed in approximately 70–80% of ALK-positive ALCL cases [19,20]. Moreover, NPM-ALK is central to the pathogenesis of ALK-positive ALCL [21]. NPM-ALK mediates tumorigenesis by exerting tyrosine kinase activity on signaling proteins involved in a number of cellular pathways, including the Jak/STAT3, MEK/ERK, and PI3K/Akt pathways, all of which promote cell proliferation, survival, and migration [20–23]. Crizotinib is a small molecule inhibitor that potently inhibits ALK activity [24]. Crizotinib was approved by the US FDA for the treatment of patients with ALK-positive non-small cell lung cancer [25]. In addition, crizotinib is being studied in multiple clinical trials for advanced solid tumors and lymphomas [26,27]. Crizotinib induces apoptosis and cell cycle arrest by downregulating the levels of phosphorylated ALK and its downstream effectors in NPM-ALK^+ ALCL cell lines [24,28] and has shown therapeutic efficacy in pediatric patients with ALK^+ ALCL [29]. Combining crizotinib with conventional chemotherapeutic agents provides antitumor activity superior to that of either approach alone [30].

Given the therapeutic potentials of anti-CD30-LDM and crizotinib in ALCL, we evaluated if their combination produced synergistic antitumor effects in ALCL cells positive for both CD30 and ALK ($CD30^+$/ALK^+) and to further explore the potential of this novel combination strategy.

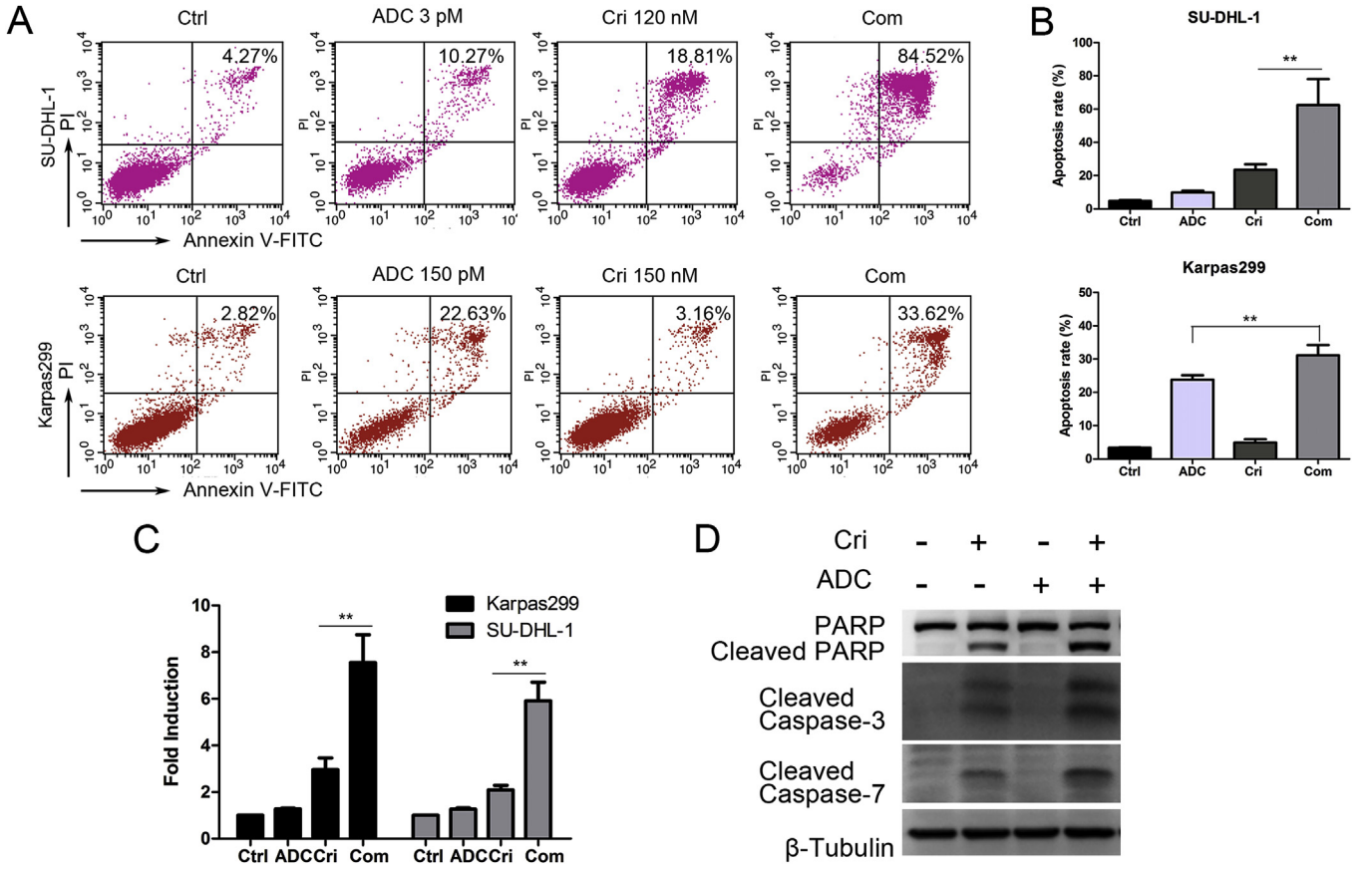

Fig. 2. Cell apoptosis induced by anti-CD30-LDM and/or crizotinib in ALK-positive ALCL cells. (A) Karpas299 and SU-DHL-1 cells were treated with anti-CD30-LDM (ADC), crizotinib (Cri), or their combination (Com) for 24 h. The cells were stained with an anti-Annexin V-FITC antibody and PI for apoptosis analysis by flow cytometry. (B) Annexin V-FITC-positive cells were defined as apoptotic. The data represent as the mean ± SD of three independent experiments; $^{**}p < 0.01$. (C) The caspase-3/-7 activity in cells treated with anti-CD30-LDM and/or crizotinib for 12 h. The fold induction of caspase-3/-7 activity was determined by comparing the activity in the treatment group with that in the untreated controls. The mean and SD of triplicate experiments are shown; $^{**}p < 0.01$. (D) The expression levels of cleaved caspase-3, caspase-7, and PARP in SU-DHL-1 cells were assessed by western blot. The treated cells were exposed to anti-CD30-LDM (3 pM) and/or crizotinib (120 nM) for 12 h.

2. Materials and methods

2.1. Cell lines

The ALCL cell lines Karpas299 and SU-DHL-1 were purchased from BioPike (Beijing, China), and the Hodgkin lymphoma-derived cell line L428 was obtained from Creative Bioarray, Inc. (Shirley, NY, USA). The Karpas299, SU-DHL-1, and L428 cell lines were cultured in RPMI 1640 medium supplemented with 10% fetal bovine serum. All cell lines were cultured in a humidified incubator (Thermo Fisher Scientific, Waltham, MA, USA) maintained at 37 °C with 5% CO_2.

2.2. Regents and antibodies

Crizotinib was purchased from J&K Chemicals (Beijing, China), and SCH77298 was purchased from Top Science Biochem (Shanghai, China). Crizotinib and SCH77298 were dissolved in dimethyl sulfoxide and stored at −80 °C. Anti-CD30-LDM was prepared in our laboratory and stored at −80 °C. Specific antibodies against ALK, NPM-ALK, phosphorylated NPM-ALK, STAT3, phosphorylated STAT3, ERK1/2, phosphorylated ERK1/2, JunB, phosphorylated JunB, p21, p53, phosphorylated p53, PARP, cleaved PARP, cleaved caspase-3, cleaved caspase-7, and β-tubulin were purchased from Cell Signaling Technology (Beverly, MA, USA). The anti-Ki-67 antibody was purchased from ZSGB-BIO Technology (Beijing, China).

2.3. Cell proliferation inhibition assays

The cell lines were seeded in 96-well plates at a density of 2.5×10^4 cells per well and incubated at 37 °C for 2 h. The cells were treated with anti-CD30-LDM and/or crizotinib at the indicated concentrations and then incubated at 37 °C for 48 h. Cell viability was measured using a Cell Counting Kit-8 (CCK-8) assay (Dojindo, Kumamoto, Japan) with a microplate reader (SpectraMax i3x, Molecular Devices, San Jose, CA, USA) at 450 nm. The data were normalized to those of the surviving fractions and compared with the data from the untreated controls. The IC_{50} was defined as the drug concentration at which the cell growth was inhibited by 50% and was determined from the dose-response curves using SPSS 16.0 software (IBM SPSS, Chicago, IL, USA).

2.4. Synergy assays

The coefficient of drug interaction (CDI) was used to analyze the synergistic or antagonistic effects of the drug combinations, as reported previously [31]. The CDI was calculated relative to the surviving fractions of each group as follows: CDI = AB/(A × B); where AB is the ratio of the optical density of the combination group to that of the control group at 450 nm, and A and B are the ratio of the optical density of each single-agent group to that of the control group at 450 nm. A CDI value $<$, $=$, or >1 indicates a synergistic, additive or antagonistic effect, respectively. CDI values < 0.7 indicated strong synergy.

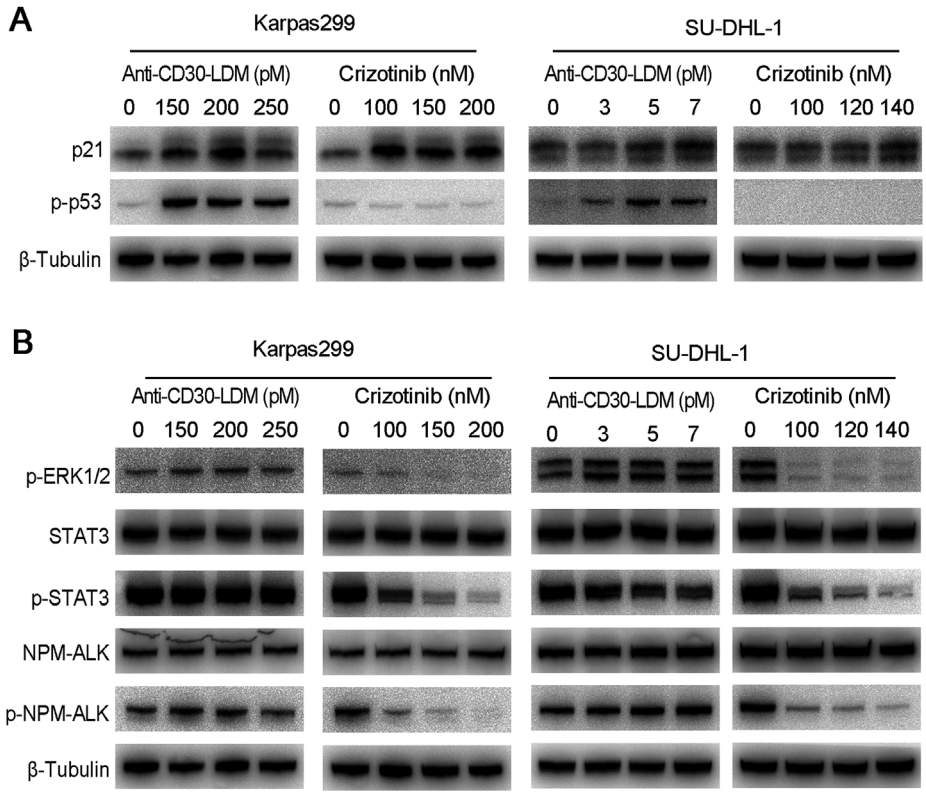

Fig. 3. Effects of anti-CD30-LDM and crizotinib on signaling pathways. To evaluate the effects of anti-CD30-LDM and crizotinib on p53-related pathways (A) and NPM-ALK-related pathways (B), Karpas299 cells were treated with anti-CD30-LDM (0, 150, 200, and 250 pM) or crizotinib (0, 100, 150 and 200 nM) and SU-DHL-1 cells were treated with anti-CD30-LDM (0, 3, 5 and 7 pM) or crizotinib (0, 100, 120 and 140 nM) for 12 h.

2.5. Apoptosis assays

Cells were plated in 6-well plates, incubated at 37 °C for 2 h, and then exposed to anti-CD30-LDM and/or crizotinib for 24 h. The cells were collected for analysis according to the manufacturer's protocol for the Annexin V-FITC Apoptosis Kit (Dojindo) and analyzed with a FACSCalibur flow cytometer (BD Biosciences, San Jose, CA, USA). Annexin V-positive cells were defined as apoptotic.

2.6. Caspase-3/-7 activity

Karpas299 and SU-DHL-1 cells were seeded at 2×10^4 cells per well in a white 96-well plate. After incubation for 2 h, the cells were treated with anti-CD30-LDM and/or crizotinib for 12 h, and caspase-3/-7 activity was measured using a Caspase-Glo 3/7 Assay Kit (Promega, Madison, WI, USA) according to the manufacturer's protocol. The luminescence signal was detected with a microplate reader (SpectraMax i3x). The increased activity of caspase-3/-7 in drug-treated samples was expressed as the fold induction relative to the activity of the untreated control.

2.7. Western blot analysis

Whole cell lysates were prepared after incubation with drugs for 12 h. The concentrations of the protein samples were quantified using a BCA protein assay kit (Thermo Fisher Scientific) according to the manufacturer's instructions. Equal amounts of protein from each sample were analyzed by SDS-PAGE and then transferred to PVDF membranes (Merck Millipore, Darmstadt, Germany). The membranes were then blocked with 5% bovine serum albumin (BSA) in TBST for 2 h at room temperature and incubated with the indicated primary antibody, diluted in 5% BSA in TBST, at 4 °C overnight. Then, the membranes were incubated with peroxidase-linked secondary antibodies for 2 h at room temperature. The protein bands were detected with an enhanced chemiluminescence kit (Merck Millipore).

2.8. Therapeutic study of the murine xenograft tumor models

For the Karpas299 xenograft model, female NOD/SCID mice were purchased from Beijing Vital River Laboratory Animal Technology Co., Ltd. (Beijing, China). Female NOD-*Prkd*^{scid}*IL2rg*^{tm1} mice were purchased from Biocytogen Jiangsu Co., Ltd. (Jiangsu, China) and used for the SU-DHL-1 xenograft model. The mice were housed under specific pathogen-free conditions. All animal experiments were approved by the Institutional Animal Care and Use Committee of the Institute of Medicinal Biotechnology, Chinese Academy of Medical Sciences. Aliquots of cells (5×10^6) were suspended in 200 μL of PBS and subcutaneously injected into the right flank of 6- to 8-week-old mice. When the average tumor volume reached 100 mm^3, the mice were randomized into six groups (n = 6 per group) and treated intravenously. The tumors were measured twice a week with calipers, and the tumor volumes were determined using the following formula: (length × width^2)/2. The tumor growth inhibition rate was calculated using the following formula: [1 - (tumor volume$_{\text{treated final}}$-tumor volume$_{\text{treated initial}}$)/(tumor volume$_{\text{control final}}$ - tumor volume$_{\text{control initial}}$)] × 100%. At the end of the experiments, the mice were euthanized. The organs and tumor tissues were harvested from the mice for histological examination and immunohistochemical analysis.

2.9. Histological examination and immunohistochemistry

Mouse tumor tissues were fixed in 10% neutral buffered formalin, dehydrated stepwise through an ascending series of alcohol solutions, and finally dewaxed in xylene. The tissues were then embedded in paraffin, sectioned at 5 μm by a microtome, and stained with hematoxylin and eosin (H&E). The expression level of Ki-67 was evaluated by immunohistochemistry in the paraffin-embedded tumor sections, according to a previously described protocol [32].

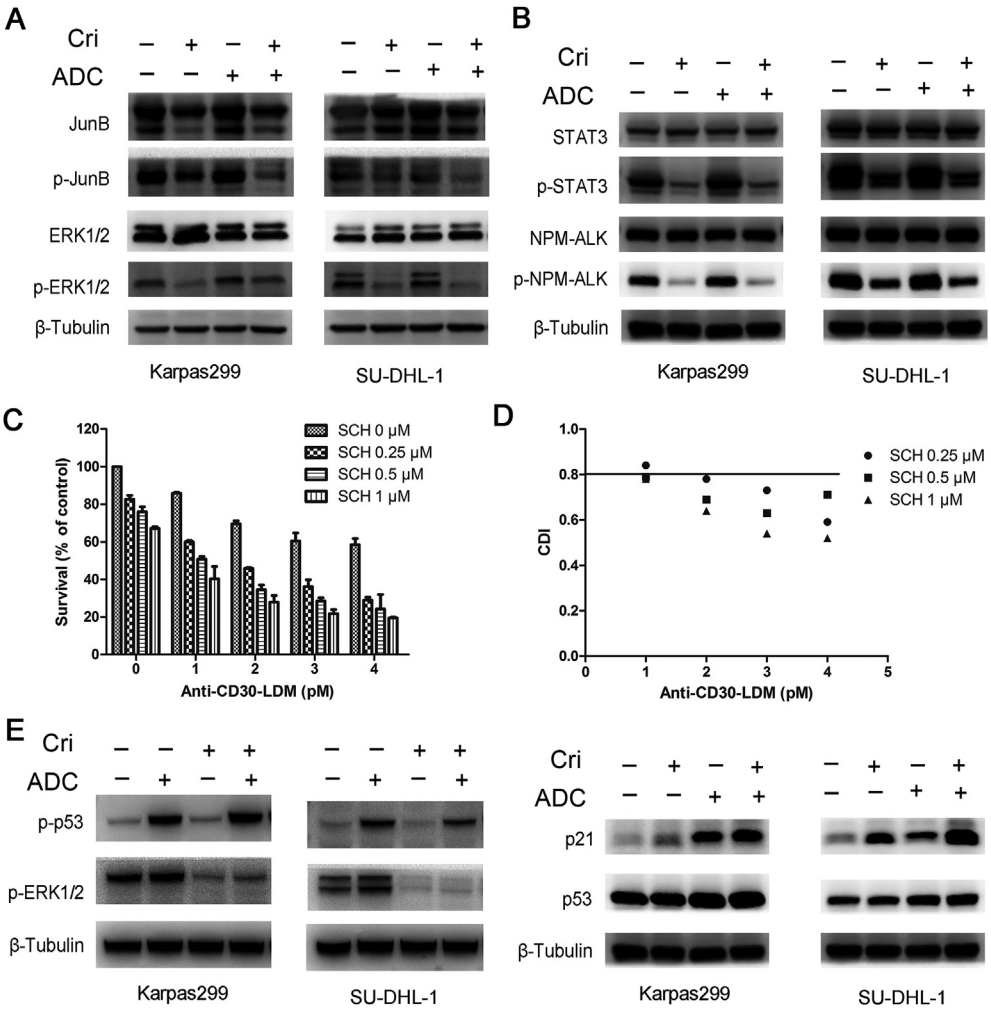

Fig. 4. Combined effects of anti-CD30-LDM and crizotinib on cell signaling pathways. (A, B, and E) Karpas299 or SU-DHL-1 cells were treated with anti-CD30-LDM (ADC, 150 pM or 3 pM, respectively) and/or crizotinib (Cri, 150 nM or 120 nM, respectively) for 12 h. Then, the cells were collected to assess the expression levels of relevant proteins. β-Tubulin was used as the loading control. (C) SU-DHL-1 cells were treated with anti-CD30-LDM (0, 1, 2, 3, and 4 pM) and/or SCH772984 (SCH, 0, 0.25, 0.5, and 1 μM) for 48 h, and cell viability was measured by a CCK-8 assay. The survival rates were calculated as the ratio of the cell survival in the treatment group to that in the control group. (D) The CDI values were calculated; CDI < 1 indicates a synergistic effect.

2.10. Statistical analysis

The data are expressed as the mean ± SD. GraphPad Prism 5.0 was used for statistical analysis. Differences between two groups were calculated using a standard *t*-test. $P < 0.05$ was considered statistically significant.

3. Results

3.1. Anti-CD30-LDM combined with crizotinib enhanced antiproliferative activity in ALK$^+$ ALCL cells

Western blot analysis revealed that the ALCL cell lines, Karpas299 and SU-DHL-1, but not the HL cell line L428, expressed the ALK and NPM-ALK proteins (Fig. 1A). To determine whether crizotinib can effectively reduce the viability of ALK-positive or ALK-negative cells, the cells were treated with increasing concentrations of crizotinib for 48 h and cell proliferation was assessed. Crizotinib inhibited cell proliferation in a dose-dependent manner, with IC_{50} values of 4.01 (± 1.01) × 10^{-7} M in Karpas299 cells and 1.59 (± 0.07) × 10^{-7} M in SU-DHL-1 cells, but had little effect on L428 cells up to the highest dose of 10 μM (Fig. 1B). Our previous work showed that anti-CD30-LDM inhibited the proliferation of SU-DHL-1, Karpas299, and L428 cells with IC_{50} values ranging from 0.59 × 10^{-11} M to 3.74 × 10^{-11} M [12]. Based on these data, we evaluated the ability of the combination regimen of anti-CD30-LDM plus crizotinib to inhibit cell proliferation in the SU-DHL-1, Karpas299, and L428 cell lines. In Karpas299 cells, the survival rate was 79.38% with 50 pM anti-CD30-LDM and 66.51% with 125 nM crizotinib, while the combination treatment resulted in a cell survival rate of 37.15% and a CDI value of 0.70. In SU-DHL-1 cells, the cell survival rate was 61.20% with 3 pM anti-CD30-LDM and 75.65% with 120 nM crizotinib, while the combination treatment resulted in a cell survival rate of 17.65% and a CDI value of 0.34. Compared with the cells treated with the single agents, SU-DHL-1 and Karpas299 cells treated with the combination regimen showed synergistic responses, with CDI values < 1. Notably, the combination regimen showed strong synergy in SU-DHL-1 cells, with CDI values ranging from 0.23 to 0.69 (Fig. 1C). Similar results were obtained when the same cells were treated with LDM/crizotinib (Fig. 1D), suggesting that the synergistic effect of the anti-CD30-LDM and crizotinib combination is mechanistically linked to the action of the LDM antibiotic. In contrast, the combination regimen did not exhibit significant inhibitory activity in the L428 cell line, with CDI values > 1 (Fig. 1E).

3.2. The combination of anti-CD30-LDM and crizotinib enhanced the apoptosis of ALCL cells

To determine whether the synergistic growth inhibition induced by the combination of anti-CD30-LDM and crizotinib was due to apoptosis, we analyzed cell apoptosis by flow cytometry. The treatment of SU-DHL-1 cells with the combination of anti-CD30-LDM and crizotinib induced a significant increase in the percentage of late apoptotic cells (84.51%) compared with the percentage observed for 3 pM anti-CD30-LDM (10.27%) or 120 nM crizotinib (4.27%) alone. In Karpas299 cells, the combined treatment led to 33.62% of late apoptotic cells, compared with 22.63% with 150 pM anti-CD30-LDM alone and 3.16% with

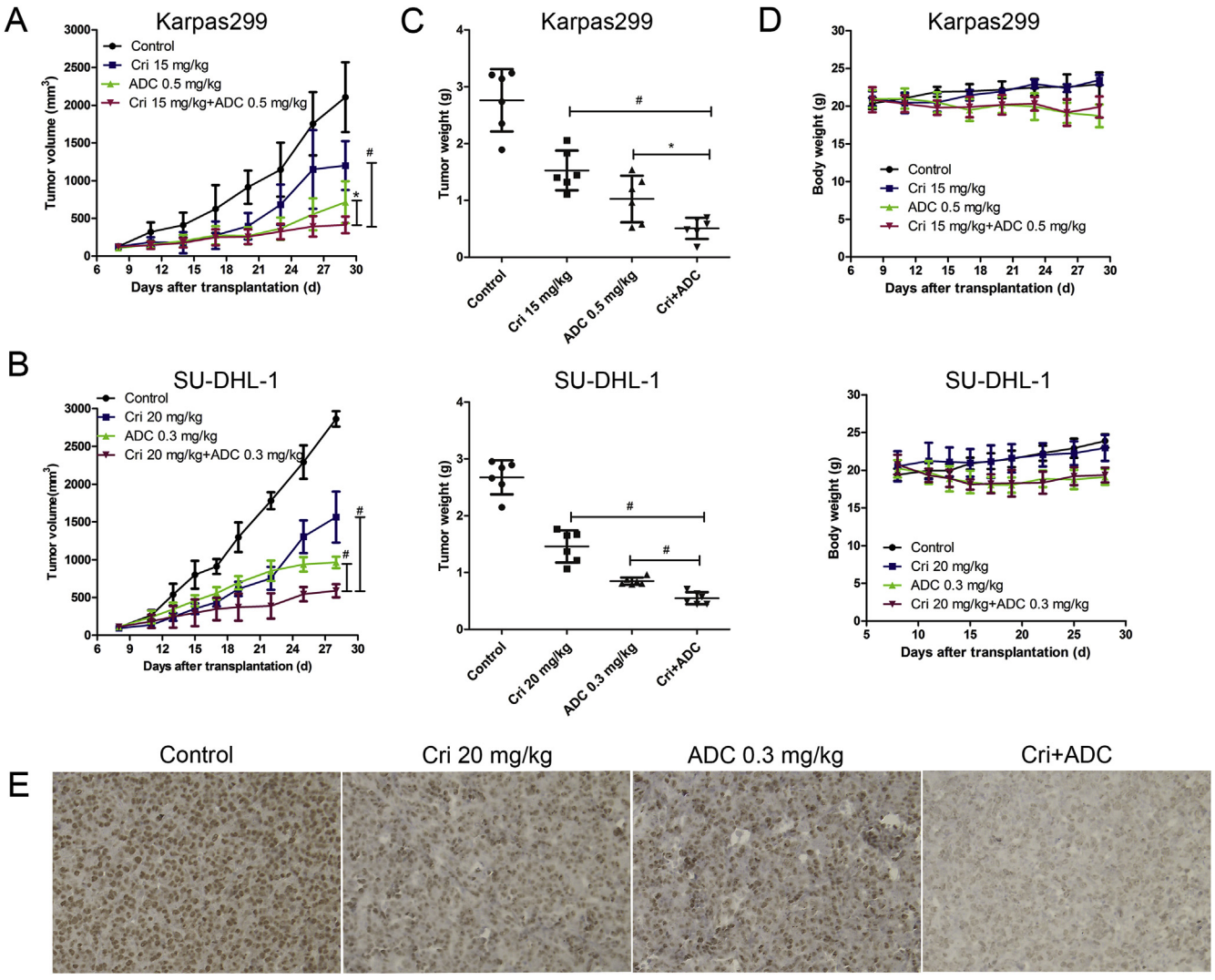

Fig. 5. Antitumor efficacy of the anti-CD30-LDM and crizotinib combination in murine xenograft models. In the Karpas299 xenograft model, the mice were treated with 15 mg/kg crizotinib (Cri) and/or 0.5 mg/kg anti-CD30-LDM (ADC). In the SU-DHL-1 xenograft model, mice were treated with 20 mg/kg crizotinib and/or 0.3 mg/kg anti-CD30-LDM. The first dose was administered on day 8. The tumor growth curves (n = 6) for the Karpas299 xenograft model (A) and the SU-DHL-1 xenograft model (B) are shown. (C) The tumor weights of the Karpas299 and SU-DHL-1 xenografts were recorded after the mice were sacrificed. (D) The changes in the mouse body weights during the experiment were recorded. The data are expressed as the mean ± SD (n = 6). *$p < 0.05$, #$p < 0.001$. (E) The expression levels of Ki-67 in the SU-DHL-1 tumor sections were evaluated by immunohistochemistry (200 ×).

150 nM crizotinib alone (Fig. 2A). The percentages of SU-DHL-1 and Karpas299 cells undergoing apoptosis were 23.43% and 4.91%, respectively, for crizotinib treatment; 9.80% and 23.82%, respectively, for anti-CD30-LDM treatment; and 62.34% and 31.09%, respectively, for the combination treatment (Fig. 2B). We also detected activation of the apoptosis markers caspase-3/-7 in Karpas299 and SU-DHL-1 cells. Anti-CD30-LDM or crizotinib alone led to modest activation of caspase-3/-7 in both cell lines after 12-h incubation. However, the combination treatment showed a markedly enhanced (greater than 2.5-fold) induction of caspase-3/-7 (Fig. 2C). Western blot analysis showed that the levels of cleaved PARP, caspase-3, and caspase-7 were increased in the combination treatment group compared with the single-agent treatment groups, further demonstrating that the combination treatment clearly enhances cell apoptosis (Fig. 2D). Collectively, these findings demonstrated that the cell growth inhibition observed with the combination treatment could be explained at least in part by the enhanced apoptotic response mediated by the caspase cascade.

3.3. Anti-CD30-LDM and crizotinib exhibited different effects on signal transduction pathways

The protein levels and phosphorylation or activation of p53 are tightly controlled under normal cell conditions. However, in response to DNA damage, p53 can become phosphorylated, leading to its activation [33]; while, p21 is a tumor suppressor gene activated by the p53 gene. To investigate this response, Karpas299 and SU-DHL-1 cells were treated with anti-CD30-LDM or crizotinib at different concentrations for 12 h and evaluated by western blot. The effects of anti-CD30-LDM on p53 phosphorylation are shown in Fig. 3A. An increase in p-p53 (Ser15) was observed in cells treated with anti-CD30-LDM compared with untreated control cells, while crizotinib alone had no effect on p-p53 levels. In addition, the expression of p21 was upregulated in both anti-CD30-LDM-treated and crizotinib-treated cells compared with control cells. One of the reported mechanisms by which crizotinib halts tumor cell growth is a decrease in the activity of signaling cascades downstream of the ALK receptor, including the STAT3 and MAPK/ERK pathways [19]. Crizotinib, but not anti-CD30-LDM, decreased the phosphorylation levels of ALK, STAT3, and ERK1/2 in Karpas299 and

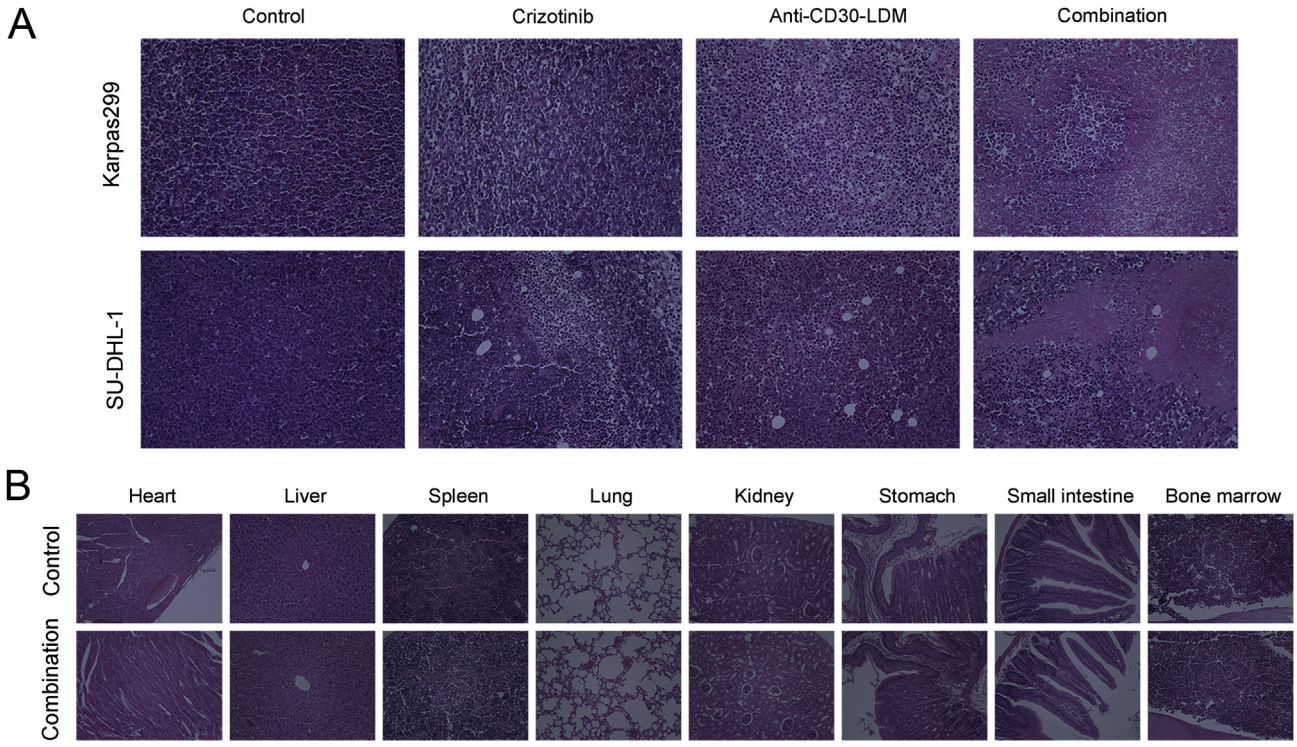

Fig. 6. H&E staining of the tumors and various organs from tumor-bearing mice. (A) Tumor slides from the Karpas299 and SU-DHL-1 xenografts were stained with H&E and analyzed. Tumor sections from mice treated with 15 mg/kg crizotinib or 0.5 mg/kg anti-CD30-LDM in the Karpas299 xenograft model and 20 mg/kg crizotinib or 0.3 mg/kg anti-CD30-LDM in the Su-DHL-1 xenograft model showed more pyknotic nuclei than those from the control groups. Tumor sections from mice treated with the combination therapy showed pyknotic cells as well as large areas of dead cells. Microscopy images are shown (200 ×). (B) The histopathological observations from various organs of the control and combination groups in the SU-DHL-1 xenograft model. No toxicopathological changes were found in the heart, liver, spleen, lungs, kidneys, stomach, small intestine or bone marrow (200 ×).

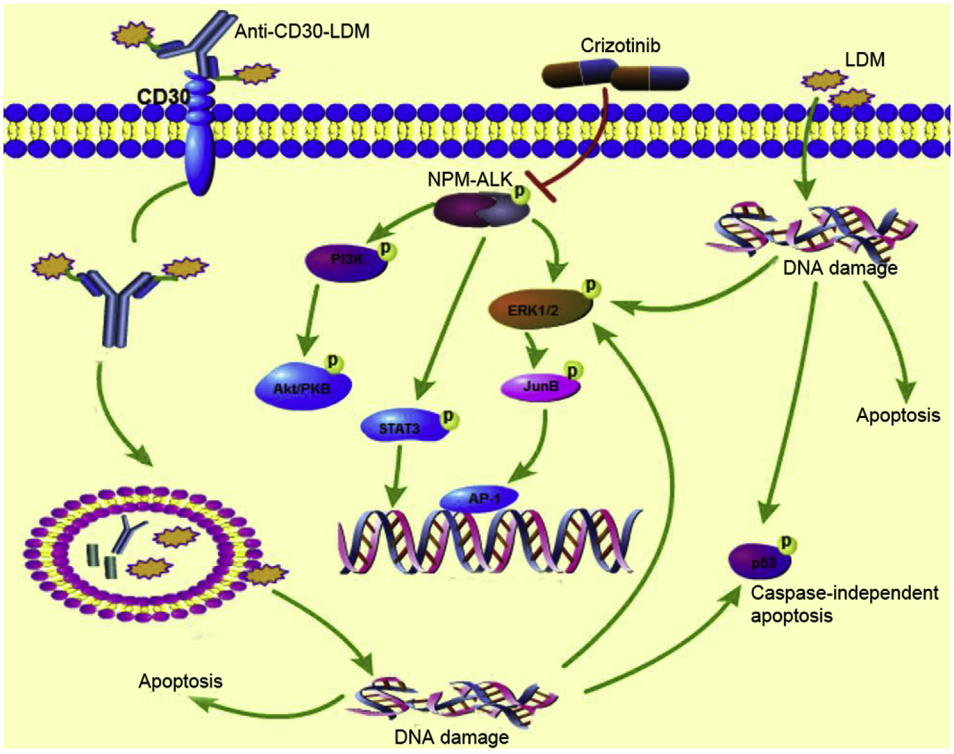

Fig. 7. Schematic diagram of the cellular responses to combination treatment with anti-CD30-LDM and crizotinib in NPM-ALK-positive ALCL cells. The figure depicts the cellular responses following DNA damage and NPM-ALK inhibition. Anti-CD30-LDM and LDM promote DNA damage. This DNA damage leads to the phosphorylation of p53 and the induction of apoptosis, while anti-CD30-LDM treatment increases the levels of phosphorylated ERK1/2, which facilitates cell proliferation and survival. Crizotinib inhibits NPM-ALK phosphorylation, leading to the inhibition of ERK1/2 phosphorylation and enhanced sensitivity of tumor cells to DNA damage. Thus, this combination of anti-CD30-LDM and crizotinib augments cell death.

SU-DHL-1 cells (Fig. 3B). In contrast, anti-CD30-LDM treatment tended to upregulate the expression levels of phosphorylated ERK1/2 in both cell lines (Fig. 3B). These data indicated that crizotinib could enhance anti-CD30-LDM-induced cell apoptosis by inhibiting the activity of ERK1/2 signaling.

3.4. Crizotinib downregulated anti-CD30-LDM-induced ERK1/2 phosphorylation and enhanced p-JunB inhibition

To determine the combined effects of anti-CD30-LDM and crizotinib on cell signaling proteins, Karpas299 and SU-DHL-1 cells were treated for 12 h with anti-CD30-LDM and crizotinib, separately and in combination. In SU-DHL-1 cells, but not Karpas299 cells, combination treatment with anti-CD30-LDM and crizotinib effectively decreased ERK1/2 phosphorylation compared with crizotinib alone (Fig. 4A). This may explain why Karpas299 cells were not as sensitive as SU-DHL-1 cells to the combination treatment in cell proliferation inhibition assays. Moreover, the combination treatment further downregulated the levels of phosphorylated JunB, which acts as a downstream signaling molecule in the MEK/ERK pathway to promote transcription (Fig. 4A). In addition, crizotinib decreased the phosphorylation levels of ALK and STAT3 in both cells, but these effects were not enhanced with the combination treatments (Fig. 4B). These data suggested that ERK1/2 signaling plays an important role in the cooperative effects of the anti-CD30-LDM and crizotinib combination. We also studied the efficacy of anti-CD30-LDM in combination with SCH772984, an inhibitor of ERK1/2 [34]. Our data showed that the survival rate of SU-DHL-1 cells under combined treatment with anti-CD30-LDM (3 pM) and SCH772984 (0.5 μM) was 27.25% compared with 63.46% with anti-CD30-LDM treatment alone and 77.86% with SCH772984 treatment alone (Fig. 4C). Surprisingly, combined treatment with anti-CD30-LDM and SCH772984 in SU-DHL-1 cells synergistically decreased the cell survival rate, with CDI values ranging from 0.52 to 0.84 (Fig. 4D). These results were similar to those for the combination of anti-CD30-LDM and crizotinib, suggesting that the inhibition of ERK1/2 induced by crizotinib can enhance the cytotoxicity of anti-CD30-LDM in SU-DHL-1 cells. Furthermore, the increase in p-p53 expression observed with anti-CD30-LDM was not altered by co-treatment with crizotinib, and the expression levels of the p53 and p21 proteins were upregulated with the combination treatment (Fig. 4E). This finding indicates that cell apoptosis was higher with the co-treatment than with the single-agent treatments. In summary, anti-CD30-LDM induced DNA damage and p53-mediated apoptosis, and was accompanied by ERK1/2 activation. However, crizotinib inhibited NPM-ALK-mediated ERK1/2 activation and sensitized cells to anti-CD30-LDM-induced DNA damage and apoptosis.

3.5. Anti-CD30-LDM combined with crizotinib decreased the growth of subcutaneous xenograft tumors in vivo

To investigate whether our *in vitro* findings could be translated in an *in vivo* setting, we evaluated the antitumor effects in mouse xenograft models using the Karpas299 and SU-DHL-1 cell lines. In the Karpas299 xenograft model, anti-CD30-LDM (0.5 mg/kg) or crizotinib (15 mg/kg) as single agents exerted moderate antitumor effects, decreasing the tumor volume by 69.35% and 45.73%, respectively. Combination treatment with anti-CD30-LDM and crizotinib further decreased the tumor volume compared with that observed with anti-CD30-LDM alone ($413.63 \pm 109.67\ mm^3$ *vs.* $714.44 \pm 253.23\ mm^3$, respectively, $p < 0.05$) and crizotinib alone ($413.63 \pm 109.67\ mm^3$ *vs.* $1199.89 \pm 324.42\ mm^3$, respectively, $p < 0.001$). Thus, the combination treatment inhibited tumor growth by 85.27% (Fig. 5A). In the SU-DHL-1 xenograft model, the tumor growth inhibition rate in the combination treatment group was 82.72%, compared with 69.12% in the anti-CD30-LDM (0.3 mg/kg) group and 46.70% in the crizotinib (20 mg/kg) group (Fig. 5B). Consistent with the measurable tumor volumes, there was a significant difference in tumor weight between the combined treatment group and the single-agent treatment groups (Fig. 5C). The treated mice tolerated the therapy, as evidenced by the lack of significant body weight loss during the treatment period (Fig. 5D).

Immunohistochemical staining to calculate the mitotic index (Ki-67 expression) in SU-DHL-1 xenografts revealed that the Ki-67 expression in the anti-CD30-LDM plus crizotinib group was decreased compared with that in the monotherapy groups, indicating the antiproliferative activity of the combination treatment (Fig. 5E). To evaluate the changes in the tumors in response to anti-CD30-LDM and/or crizotinib, the tumor tissue samples were stained with H&E. In both the Karpas299 and SU-DHL-1 xenografts, anti-CD30-LDM or crizotinib alone induced cell apoptosis, as evidenced by the increased number of pyknotic nuclei in the monotherapy groups compared with the control groups; furthermore, the tumor sections from the combination treatment group showed not only pyknotic cells but also large areas of dead cells (Fig. 6A).

To observe changes in the organs in response to anti-CD30-LDM and/or crizotinib, the organs of the SU-DHL-1 xenograft model mice were stained with H&E to evaluate the *in vivo* toxicity of the treatments. Compared with the control group, the heart, liver, spleen, lungs, kidneys, stomach, small intestine, and bone marrow of mice treated with the anti-CD30-LDM and crizotinib combination showed no toxicopathological changes, suggesting this therapeutic regimen has negligible toxicity *in vivo* (Fig. 6B). Consistent with the findings from the *in vitro* experiments, the results from the *in vivo* experiments support the promising antitumor activity of the combination of anti-CD30-LDM and crizotinib.

4. Discussion

Given the common mutability of cancers, combination therapies targeting at least two different pathways may overcome cancer drug resistance and achieve better antitumor efficacy [35]. Furthermore, optimizing the effectiveness of combination therapies, especially combinations of ADCs with small molecule inhibitors, in preclinical research remains an important objective and advanced strategy in ADC development. Investigators have attempted to mechanistically combine drugs of various modalities. For example, the efficacy of BV in human HL is augmented when it is combined with ruxolitinib, a JAK1/2 inhibitor [16]. Similarly, PI3K/mTOR inhibitors enhanced the antitumor activity of an anti-5T4 ADC [15] and MAPK pathway inhibitors sensitized BRAF-mutant melanoma with a GPNMB-targeting ADC [36]. We previously described the development of a novel DNA-damaging ADC, anti-CD30-LDM, and its antitumor activity in a CD30-positive ALCL xenograft model.

Here, we provided further evidence for the antitumor effects of anti-CD30-LDM by combining it with the ALK inhibitor crizotinib. Surprisingly, the results showed that the drugs cooperatively induced cell apoptosis and inhibited tumor growth. Notably, the combination of either anti-CD30-LDM or LDM with crizotinib showed similar synergistic inhibitory effects on cell proliferation in the ALK-positive Karpas299 and SU-DHL-1 cell lines, while the combination strategy showed no synergistic or additive effects in the ALK-negative L428 cell line. This result was in accordance with the observations that crizotinib significantly inhibits the expression of phosphorylated NPM-ALK, leading to cell death, and has a minimal cytotoxic effect on ALK-negative cells.

NPM-ALK is a constitutively activated protein tyrosine kinase that possesses substantial oncogenic potential [37]. To induce an oncogenic effect, NPM-ALK activates several downstream proteins that regulate cell survival and growth [38]. Our results demonstrated that the phosphorylation of NPM-ALK was reduced dramatically after treatment with crizotinib in Karpas299 and SU-DHL-1 cells. Subsequently, downstream ERK1/2 phosphorylation was inhibited in response to the

decreased phosphorylation of NPM-ALK. In contrast, the induction of DNA strand breaks in both cell lines after treatment with anti-CD30-LDM was followed by or occurred with the upregulation of ERK1/2 phosphorylation. The activation of ERK1/2 is thought to be an important factor in suppressing apoptosis and promoting cell proliferation [39]. However, the effects of the MER-ERK cascade on modulating the DNA damage response are conflicting. Inhibition of ERK1/2 activity attenuated DNA damage-induced cell cycle arrest and apoptosis in several mammalian cell lines, including NIH3T3, MEF, MCF-7, HCT116, and HeLa [40–43]. Yet, inhibition of ERK1/2 activity facilitated DNA damage-induced apoptosis in U266 (a human multiple myeloma cell line), HL60 (an acute myelogenous leukemia cell line) and NB4 (an acute promyelocytic leukemia cell line) cells [44,45]. Therefore, we speculated that the inhibition of ERK1/2 activation may enhance the efficacy of DNA-damaging drugs in tumors of hematopoietic and lymphoid tissues. We used a potent and noncompetitive inhibitor of ERK1/2, SCH772984, to validate this hypothesis [34]. As expected, our data showed that the combination of anti-CD30-LDM and SCH772984 synergistically decreased the cell survival rate and enhanced cell death in SU-DHL-1 cells. Similar to this combination therapy, crizotinib inhibited ERK1/2 phosphorylation, which was increased to facilitate cell survival during treatment with anti-CD30-LDM. Thus, combination treatment with anti-CD30-LDM and crizotinib showed a synergistic inhibitory effect on cell proliferation in ALK^+ ALCL cells (Fig. 7).

The ability of cells to repair DNA damage to maintain their genomic integrity is an important determinant of treatment efficacy. DNA strand damage by anti-CD30-LDM initiates DNA repair and the phosphorylation of several target proteins, including the tumor suppressor p53. The phosphorylation of p53 (Ser15) has been reported to result from DNA damage induced by treatment with cisplatin or isomerase I or II inhibitors [46]. The p53 protein was phosphorylated at the Ser15 site with both anti-CD30-LDM treatment and the combination treatment; however, the level of phosphorylated p53 seen with the combination treatment was not higher than that seen with the anti-CD30-LDM treatment alone. High levels of p53-induced p21 are correlated with cell cycle arrest and DNA damage [47]. Interestingly, p21 expression was significantly upregulated with the combination treatment compared with that observed with the single-agent treatments. In addition, the combination treatment increased PARP, caspase-7, and caspase-3 cleavage to promote the activation of proapoptotic mediators. These increased cleavage levels were likely due to enhanced DNA damage and further cell death.

ALCL is a highly aggressive hematologic malignancy and effective therapeutic strategies that minimize toxicity to the patient are needed. Our data contribute to this growing field by showing that crizotinib, an NPM-ALK inhibitor, and anti-CD30-LDM, a DNA damage-related ADC, cooperatively inhibit cancer cell proliferation and tumor growth. In addition, we found that the enhanced antitumor effect of the combination treatment was mediated at least in part by inhibiting DNA damage-related ERK1/2 signaling. Furthermore, in both the Karpas299 and SU-DHL-1 xenograft models, the tumor growth in the groups treated with the combination of anti-CD30-LDM and crizotinib was significantly inhibited compared with that in the monotherapy groups. In summary, our data unequivocally indicate the beneficial effects of anti-CD30-LDM and crizotinib in $CD30^+/ALK^+$ ALCL and suggest that the pharmacological inhibition of NPM-ALK in the presence of DNA-damaging agents might be effective in the treatment of NPM-ALK-positive tumors. This study provided scientific support for the clinical evaluation of anti-CD30-LDM or other DNA-damaging agents, combined with NPM-ALK inhibitors, as well as a potential rational strategy for targeted combination therapy in ALCL.

Conflicts of interest

All authors declare no conflict of interests.

Author contributions

R.W. and L.L. conducted experiments, analyzed the available data and wrote the manuscript. A.J.D. performed part of the western blot analysis. X.J.L. provided support for the animal studies. Y.L. performed the H&E staining and immunohistochemical analysis. Q.F.M., J.H.G., and Y.S.Z. conceptualized the framework for this research and guided the study work. All authors helped edit the manuscript.

Acknowledgements

This work was supported by the CAMS Innovation Fund for Medical Sciences (CIFMS, 2016-I2M-3-013) and 'Significant New Drug Development' Major Science and Technology Development Projects of China (No. 2013ZX09103003-008).

References

[1] M. Boi, E. Zucca, G. Inghirami, F. Bertoni, Advances in understanding the pathogenesis of systemic anaplastic large cell lymphomas, Br. J. Haematol. 168 (2015) 771–783.
[2] S.D. Turner, L. Lamant, L. Kenner, L. Brugieres, Anaplastic large cell lymphoma in paediatric and young adult patients, Br. J. Haematol. 173 (2016) 560–572.
[3] B. Pro, R. Advani, P. Brice, N.L. Bartlett, J.D. Rosenblatt, T. Illidge, et al., Brentuximab vedotin (SGN-35) in patients with relapsed or refractory systemic anaplastic large-cell lymphoma: results of a phase II study, J. Clin. Oncol. 30 (2012) 2190–2196.
[4] H. Muta, E.R. Podack, CD30: from basic research to cancer therapy, Immunol. Res. 57 (2013) 151–158.
[5] S. Dabir, A. Kresak, M. Yang, P. Fu, G. Wildey, A. Dowlati, CD30 is a potential therapeutic target in malignant mesothelioma, Mol. Canc. Therapeut. 14 (2015) 740–746.
[6] J. Chen, Y. Zhang, M.N. Petrus, W. Xiao, A. Nicolae, M. Raffeld, et al., Cytokine receptor signaling is required for the survival of ALK- anaplastic large cell lymphoma, even in the presence of JAK1/STAT3 mutations, Proc. Natl. Acad. Sci. U.S.A. 114 (2017) 3975–3980.
[7] A.A. Hombach, A. Görgens, M. Chmielewski, F. Murke, J. Kimpel, B. Giebel, et al., Superior therapeutic index in lymphoma therapy: CD30+ CD34+ hematopoietic stem cells resist a chimeric antigen receptor T-cell attack, Mol. Ther. 24 (2016) 1423–1434.
[8] A. Younes, CD30-targeted antibody therapy, Curr. Opin. Oncol. 23 (2011) 587–593.
[9] R. Chen, J. Hou, E. Newman, Y. Kim, C. Donohue, et al., CD30 downregulation, MMAE resistance, and MDR1 upregulation are all associated with resistance to brentuximab vedotin, Mol. Canc. Therapeut. 14 (2015) 1376–1384.
[10] R.G. Shao, Y.S. Zhen, Enediyne anticancer antibiotic lidamycin: chemistry, biology and pharmacology, Anti Cancer Agents Med. Chem. 8 (2008) 123–131.
[11] Y.J. Xu, Y.S. Zhen, I.H. Goldberg, C1027 chromophore, a potent new enediyne antitumor antibiotic, induces sequence-specific double-strand DNA cleavage, Biochemistry 33 (1994) 5947–5954.
[12] R. Wang, L. Li, S.H. Zhang, Y. Li, X.F. Wang, Q.F. Miao, et al., A novel enediyne-integrated antibody-drug conjugate shows promising antitumor efficacy against CD30(+) lymphomas, Mol. Oncol. 12 (2018) 339–355.
[13] M.Q. Sha, X.L. Zhao, L. Li, L.H. Li, Y. Li, T.G. Dong, et al., EZH2 mediates lidamycin-induced cellular senescence through regulating p21 expression in human colon cancer cells, Cell Death Dis. 7 (2016) e2486.
[14] T.A. Beerman, L.S. Gawron, S. Shin, B. Shen, M.M. McHugh, C-1027, a radiomimetic enediyne anticancer drug, preferentially targets hypoxic cells, Cancer Res. 69 (2009) 593–598.
[15] B. Shor, J. Kahler, M. Dougher, J. Xu, M. Mack, E. Rosfjord, et al., Enhanced antitumor activity of an anti-5T4 antibody-drug conjugate in combination with PI3K/mTOR inhibitors or taxanes, Clin. Cancer Res. 22 (2016) 383–394.
[16] W. Ju, M. Zhang, K.M. Wilson, M.N. Petrus, R.N. Bamford, X. Zhang, et al., Augmented efficacy of brentuximab vedotin combined with ruxolitinib and/or Navitoclax in a murine model of human Hodgkin's lymphoma, Proc. Natl. Acad. Sci. U.S.A. 113 (2016) 1624–1629.
[17] W.S. Huang, S. Liu, D. Zou, M. Thomas, Y. Wang, T. Zhou, et al., Discovery of brigatinib (AP26113), a phosphine oxide-containing, potent, orally active Inhibitor of anaplastic lymphoma kinase, J. Med. Chem. 59 (2016) 4948–4964.
[18] K.J. Savage, N.L. Harris, J.M. Vose, F. Ullrich, E.S. Jaffe, J.M. Connors, et al., ALK-anaplastic large-cell lymphoma is clinically and immunophenotypically different from both ALK+ ALCL and peripheral T-cell lymphoma, not otherwise specified: report from the International Peripheral T-Cell Lymphoma Project, Blood 111 (2008) 5496–5504.
[19] O. Molavi, N. Samadi, C. Wu, A. Lavasanifar, R. Lai, Silibinin suppresses NPM-ALK, potently induces apoptosis and enhances chemosensitivity in ALK-positive anaplastic large cell lymphoma, Leuk. Lymphoma 57 (2016) 1154–1162.
[20] R. Chiarle, C. Voena, C. Ambrogio, R. Piva, G. Inghirami, The anaplastic lymphoma kinase in the pathogenesis of cancer, Nat. Rev. Canc. 8 (2008) 11–23.
[21] H.M. Amin, R. Lai, Pathobiology of ALK+ anaplastic large-cell lymphoma, Blood 110 (2007) 2259–2267.

[22] M. Ceccon, M.E.B. Merlo, L. Mologni, T. Poggio, L.M. Varesio, M. Menotti, et al., Excess of NPM-ALK oncogenic signaling promotes cellular apoptosis and drug dependency, Oncogene 35 (2016) 3854–3865.
[23] P.B. Staber, P. Vesely, N. Haq, R.G. Ott, K. Funato, I. Bambach, et al., The oncoprotein NPM-ALK of anaplastic large-cell lymphoma induces JUNB transcription via ERK1/2 and JunB translation via mTOR signaling, Blood 110 (2007) 3374–3383.
[24] F.S. Hamedani, M. Cinar, Z. Mo, M.A. Cervania, H.M. Amin, S. Alkan, Crizotinib (PF-2341066) induces apoptosis due to downregulation of pSTAT3 and BCL-2 family proteins in NPM-ALK(+) anaplastic large cell lymphoma, Leuk. Res. 38 (2014) 503–508.
[25] H. QIan, F. Gao, H. Wang, F. Ma, The efficacy and safety of crizotinib in the treatment of anaplastic lymphoma kinase-positive non-small cell lung cancer: a meta-analysis of clinical trials, BMC Canc. 14 (2014) 683–688.
[26] Y.P. Mosse, S.D. Voss, M.S. Lim, D. Rolland, C.G. Minard, E. Fox, et al., Targeting ALK with crizotinib in pediatric anaplastic large cell lymphoma and inflammatory myofibroblastic tumor: a children's oncology group study, J. Clin. Oncol. 35 (2017) 3215–3221.
[27] Y.P. Mosse, M.S. Lim, S.D. Voss, K. Wilner, K. Ruffner, J. Laliberte, et al., Safety and activity of crizotinib for paediatric patients with refractory solid tumours or anaplastic large-cell lymphoma: a Children's Oncology Group phase 1 consortium study, Lancet Oncol. 14 (2013) 472–480.
[28] J.G. Christensen, H.Y. Zou, M.E. Arango, Q. Li, J.H. Lee, S.R. McDonnell, et al., Cytoreductive antitumor activity of PF-2341066, a novel inhibitor of anaplastic lymphoma kinase and c-Met, in experimental models of anaplastic large-cell lymphoma, Mol. Canc. Therapeut. 6 (2007) 3314–3322.
[29] C.G. Passerini, F. Farina, A. Stasia, S. Redaelli, M. Ceccon, L. Mologni, et al., Crizotinib in advanced, chemoresistant anaplastic lymphoma kinase-positive lymphoma patients, J. Natl. Cancer 106 (2014) djt378.
[30] K. Krytska, H.T. Ryles, R. Sano, P. Raman, N.R. Infarinato, T.D. Hansel, et al., Crizotinib synergizes with chemotherapy in preclinical models of neuroblastoma, Clin. Cancer Res. 22 (2016) 948–960.
[31] J.T. Liu, W.C. Li, S. Gao, F. Wang, X.Q. Li, H.Q. Yu, et al., Autophagy inhibition overcomes the antagonistic effect between gefitinib and cisplatin in epidermal growth factor receptor mutant non-small-cell lung cancer cells, Clin. Lung Cancer 16 (2015) e55–66.
[32] R. Wan, Y. Mo, Z. Zhang, M. Jiang, S. Tang, Q. Zhang, Cobalt nanoparticles induce lung injury, DNA damage and mutations in mice, Part. Fibre Toxicol 14 (2017) 38.
[33] C.W. Espelin, S.C. Leonard, E. Geretti, T.J. Wickham, B.S. Hendriks, Dual HER2 targeting with trastuzumab and liposomal-encapsulated doxorubicin (MM-302) demonstrates synergistic antitumor activity in breast and gastric cancer, Cancer Res. 76 (2016) 1517–1527.
[34] D.J. Wong, L. Robert, M.S. Atefi, A. Lassen, G. Avarappatt, M. Cerniglia, et al., Antitumor activity of the ERK inhibitor SCH722984 against BRAF mutant, NRAS mutant and wild-type melanoma, Mol. Canc. 13 (2014) 194.
[35] L.J. Diaz, R.T. Williams, J. Wu, I. Kinde, J.R. Hecht, J. Berlin, et al., The molecular evolution of acquired resistance to targeted EGFR blockade in colorectal cancers, Nature 486 (2012) 537–540.
[36] A.A. Rose, M.G. Annis, D.T. Frederick, M. Biondini, Z. Dong, L. Kwong, et al., MAPK pathway inhibitors sensitize BRAF-mutant melanoma to an antibody-drug conjugate targeting GPNMB, Clin. Cancer Res. 22 (2016) 6088–6098.
[37] P. Shi, R. Lai, Q. Lin, A.S. Iqbal, L.C. Young, L.W. Kwak, et al., IGF-IR tyrosine kinase interacts with NPM-ALK oncogene to induce survival of T-cell ALK+ anaplastic large-cell lymphoma cells, Blood 114 (2009) 360–370.
[38] L. Hu, X. Zhang, J. Wang, S. Wang, H.M. Amin, P. Shi, Involvement of oncogenic tyrosine kinase NPM-ALK in trifluoperazine-induced cell cycle arrest and apoptosis in ALK(+) anaplastic large cell lymphoma, Hematology 23 (2018) 284–290.
[39] S. Meloche, J. Pouyssegur, The ERK1/2 mitogen-activated protein kinase pathway as a master regulator of the G1- to S-phase transition, Oncogene 26 (2007) 3227–3239.
[40] D. Tang, D. Wu, A. Hirao, J.M. Lahti, L. Liu, B. Mazza, et al., ERK activation mediates cell cycle arrest and apoptosis after DNA damage independently of p53, J. Biol. Chem. 277 (2002) 12710–12717.
[41] Y. Yan, C.P. Black, K.H. Cowan, Irradiation-induced G2/M checkpoint response requires ERK1/2 activation, Oncogene 26 (2007) 4689–4698.
[42] D. Wu, B. Chen, K. Parihar, L. He, C. Fan, J. Zhang, et al., ERK activity facilitates activation of the S-phase DNA damage checkpoint by modulating ATR function, Oncogene 25 (2006) 1153–1164.
[43] C. Sheridan, G. Brumatti, M. Elgendy, M. Brunet, S.J. Martin, An ERK-dependent pathway to Noxa expression regulates apoptosis by platinum-based chemotherapeutic drugs, Oncogene 29 (2010) 6428–6441.
[44] Y. Dai, S. Chen, X.Y. Pei, J.A. Almenara, L.B. Kramer, C.A. Venditti, et al., Interruption of the Ras/MEK/ERK signaling cascade enhances Chk1 inhibitor-induced DNA damage in vitro and in vivo in human multiple myeloma cells, Blood 112 (2008) 2439–2449.
[45] C. Nishioka, T. Ikezoe, J. Yang, A. Yokoyama, Inhibition of MEK signaling enhances the ability of cytarabine to induce growth arrest and apoptosis of acute myelogenous leukemia cells, Apoptosis 14 (2009) 1108–1120.
[46] Y. Ling, C. Xu, L. Luo, J. Cao, J. Feng, Y. Xue, et al., Novel beta-carboline/hydroxamic acid hybrids targeting both histone deacetylase and DNA display high anticancer activity via regulation of the p53 signaling pathway, J. Med. Chem. 58 (2015) 9214–9227.
[47] H.W. Yang, M. Chung, T. Kudo, T. Meyer, Competing memories of mitogen and p53 signalling control cell-cycle entry, Nature 549 (2017) 404–408.